Low and medium power full-scale atrium fire tests and numerical validation of FDS

Cándido Gutiérrez-Montes [a], Enrique Sanmiguel-Rojas [a], Antonio Viedma b, Guillermo Rein [c]

[a]Fluid Dynamics Division of the Department of Mining and Mechanical Engineering, University of Jaen, Jaen, Spain
[b]Department of Thermal and Fluid Engineering, Technical University of Cartagena, Murcia, Spain
[c]BRE Centre for Fire Safety Engineering, The University of Edinburgh, EH9 3JL, UK

Abstract

The inclusion of atria within modern large buildings is relative recent. These structures are important architectonical features since the 60's. Atria are a source of discussion within the fire science community. They introduce complex designs and non conventional architectonical elements that can lead to fire environments diverging from those in current codes. Because of this, the current trend in fire safety in atria is towards performance based design. At this point, it is still necessary to improve and validate the existing numerical models. For this aim, some tests were carried out at the Murcia Fire Facility. These consist of 19 full-scale fire tests that provide with new experimental data of atrium fires. The fire size, the smoke extraction rate and make-up openings size and location were varied. At the present paper, a set of results from some of these experiments in a 20 m cubic facility are reported and discussed. Additionally, comparisons with the predicted results from Fire Dynamics Simulator (FDS) v.4 are also presented. FDS has turned out to be capable to predict the transient fire-induced conditions inside the facility accurately, above all at the upper parts. The predicted smoke layer descent has been also compared with the experimental one with good agreement.

1.- Introduction

In modern, industrialized and technologically developed societies, such as ours, there is a growing concern about risks prevention, security improvement, optimized designs and energy saving. Thus, the fire prevention and protection, as well as the design of fire safe buildings, are of great importance. In his work, Cox [1] concluded that the costs originated by fires among the developed countries represented the 1 % of their gross domestic product. Besides, the smoke and high temperatures induced by a fire threaten the lives of the occupants of the building, being the smoke the main cause of deaths in case of fire. Therefore, the study of fire is justified mainly in terms of security and economy, being of huge interest the researches focused on fire threatens, fire effects, fire mitigation and fire prevention [2].

The present work is focused on the study of fires within big volume interior enclosures buildings, which will be commonly named atrium from now on. This kind of structure has become a common element in modern architecture [3] and can be found in high-rise buildings, auditoria, shopping centres, airports and mass transport stations, among others.

However, the atrium represents a non conventional architectonical element that can lead to fire environments diverging significantly from those used in the development of current codes and standards [4]. Atria are a source of discussion in the fire safety community as such spaces present a challenge for the fire protection engineers because their height decreases the effectiveness of automatic sprinkler systems [5] and because they lack the floor-to-floor separations that can limit the likelihood of fire and smoke spreading from the floor of fire origin to other areas of the building [6]. Furthermore, evacuation routes in atria are of greatest concern because they become vulnerable to smoke spreading [7]. Thus, it is of great importance to know how a fire that takes place inside one of these structures develops and the effects and hazards that it can cause.

Since the 80’s, fires within atria started to be studied, both experimentally and numerically [8, 9]. In that respect, testing in full-scale enclosures [10, 11] is too complex, expensive and labour intensive, which involves a small number of tests carried out. With reduced-scale testing [12] it has to be taken into account its limitations [13]. Another alternative is the use of advanced computer models [14, 15]. It is because of the subsequent improved understanding on fire dynamics and smoke management together with the increased computing power available nowadays and the improvements and developments of the existing numerical codes, that there is a current international trend in fire protection engineering regulations towards performance-based design and risk-informed analysis [16], which relies greatly on numerical modelling.

Because of the shift towards performance-based codes and the difficulty of testing in atria, fire models are increasingly being used for developing fire safety engineering solutions [17, 18]. However, it is needed to generate more reliable and comprehensive full-scale tests to

continue with the developments, improvements and validations of the existing fire models [19] in the search for more robust and accurate tools for fire research and fire safe structures design [20].

Under the current situation, this work aims to provide with a set of full-scale experimental data of atrium fires as well as to check the capability of a numerical code (FDS) to simulate the fire environment induced in this kind of building. In all, experimental results from three tests, in which natural and mixed ventilation have been considered, are presented. Additionally, CFD simulations of these tests have been performed. Finally, the most important results and numerical vs. experimental comparisons are shown.

2.- Murcia Fire Atrium

The experimental facility used in this study is the "Fire Atrium" [21] located at the Centro Tecnológico del Metal, in Murcia, Spain, figure 1. This full-scale burning facility consists of a prismatic structure of 19.5 m x 19.5 m x 17.5 m and a pyramidal shaped roof 2.5 m tall. The walls and roof are made of 6 mm thick steel and the ground is made of concrete. There are 4 exhaust fans installed on the roof, each with a diameter of 0.56 m. There are 8 grilled vents arranged at the lower parts of the walls. Each vent has dimensions of 4.875 m x 2.5 m. A drawing of the rig with dimensions is shown in figure 2.

Fig. 1. The "Fire Atrium" of the Technological Metal Centre, Murcia, Spain.

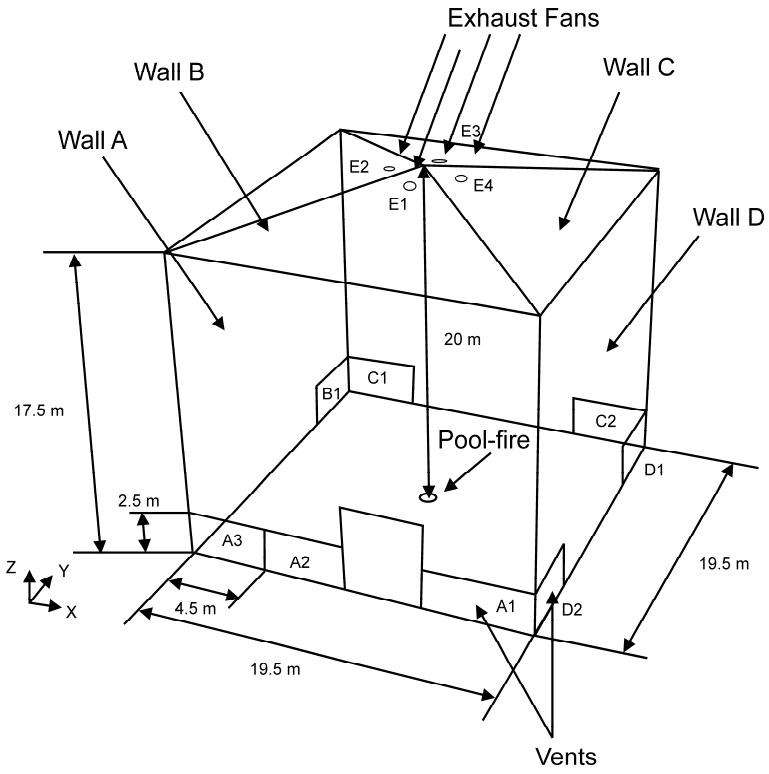

Fig. 2. Drawing and dimensions of the experimental facility "Fire Atrium".

In order to study the fire-induced thermal and flow fields, sixty one sensors have been installed measuring gas phase, walls and roof temperatures, as well as pressure drop at exhaust fans and flow velocities at the vents. To measure plume temperature, type K thermocouples and 3 mm-diameter bare and sheathed thermocouples have been installed at the same locations to assure robustness of the recordings. For the rest of gas temperature measurements (near walls and vents), 6 mm diameter class B bare Pt100 thermistor probes have been used. To measure surface temperature, 6 mm diameter type K thermocouples have been used. Differential pressure transmitters were installed to measure flow at the exhaust fans. At the vents, hot wire anemometers have been used to measure air velocity, with a range up to 2 m/s. A Modicom TSX Premium automaton connected to a PC was used to register the data with a frequency of 5 Hz. Two video cameras were also installed to monitor the flame shape and height.

Weather conditions have been measured by means of a meteorological station monitoring outside temperature, humidity and pressure. Wind velocity was also measured by means of an anemometer.

The radiation effect on temperature measurements has been neglected as the average errors are very small (lower than 5%), even in the worst case scenario of high temperatures (lower than 10%), as reported in [22].

Figure 3 summarizes the location of the main sensors considered in this work (see [21] for details).

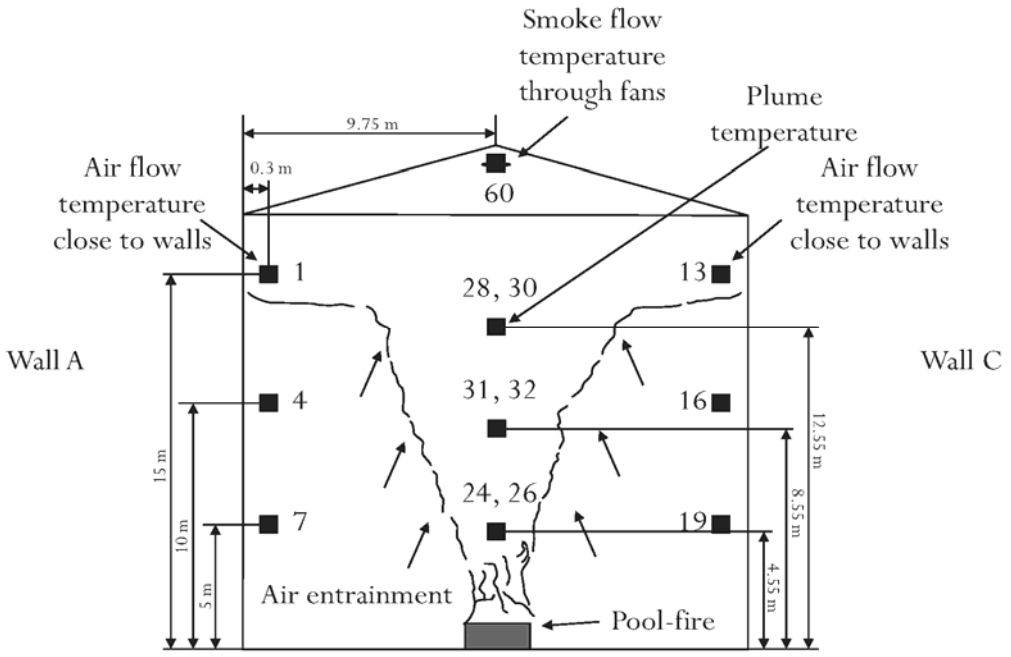

Fig. 3. Scheme of the layout of the main numbered sensors considered. View of central section from Wall D. Sensors 1, 4, 7, 13, 16, 19 and 60 are Pt100 thermistors and sensors 24, 26, 28, 30, 31 and 32 are type K thermocouples.

In addition, the mass loss of fuel in the pool was measured, as explain in section 3 of this paper.

An uncertainty analysis for the measurements was conducted (see [21] for details). The analysis shows that the total experimental uncertainty for the thermocouples is 1.5 %, that for the thermistors is 0.4 %, for the velocity probes is 4 %, for the mass flow across the fans is 10 % and for the mass loss is 1 %.

3.- Description of Fire Experiments

Results from three atrium fire tests conducted on the 4th and 7th of April 2008 are presented. The burning fuel was heptane contained in circular steel pans placed at the centre of the atrium floor. The pans were 0.25 cm deep. Two different diameters pool-fires were used, 0.92 m in the first test and 1.17 m in the last two tests. In all the tests, a layer of 2 cm of water was added to the pan before the heptane was poured to insulate the metal from the burning pool heat, thus providing a more stable steady burning regime. At the end of each test, the volume of water was measured again to confirm that no water had been lost. A summary of the principal laboratory and ambient conditions during the tests is presented in Table 1.

Fire test	Pool diameter (m)	Volume of heptane (l)	Burning time (s)	Venting conditions		Ambient conditions		Wind speed (m/s)	Calculated average HRR (MW)
				Open vents	fans on	Temp. (ºC)	Pressure (mbar)		
Test 1	0.92	52	1010	A1, A3, C1, C2 100%	E2, E4	13.0	1014	0.00	1.32
Test 2	1.17	75	843	A1, A3, C1, C2 100%	E2, E4	18.0	1014	0.85 – 1.00	2.28
Test 3	1.17	100	1094	A1, A3, C1, C2 100%	None	16.0	997	0.00 – 0.75	2.34

Table 1. Summary of laboratory and ambient conditions during the Fire Tests.

The heat release rate (HRR), $\dot{Q}$, is the most important variable to characterize a fire. For these experiments, it is calculated as

$$\dot{Q}(t) = \dot{m}(t)\chi_{eff}\Delta H_c . \quad (1)$$

where $\dot{m}$ is the mass loss rate of the fuel, ΔH_c is the heat of combustion and χ_{eff} the combustion efficiency. The heat of reaction of heptane for complete combustion is 44.6 MJ/kg [7]. The combustion efficiency expresses the difference between theoretical heat of combustion and the effective heat of combustion. It generally depends on the fuel, the soot production, the ventilation conditions and the flame size [7]. Experimental results in [23] show that χ_{eff} for well-ventilated pool-fires is weakly dependent on pool-fire diameter within the range of 0.1 – 2 m. Hostikka *et al.* [11] reported a value of 0.8 ± 0.1 for well-ventilated heptane fires ranging from 0.71 m to 1.60 m in diameter. In [19], a combustion efficiency of 0.85 ± 0.12 is suggested for heptane fires of 1.2 to 1.6 m in diameter. Based on these results, for the present work, a combustion efficiency of 0.85 is chosen.

The instantaneous mass loss rate, $\dot{m}(t)$, was not measured directly due to the weight limitation of the available balance. Instead, the average mass loss rate, $\overline{\dot{m}}$, for each test was measured as the total mass of fuel burnt divided by the burning time. The evolution of the instantaneous mass loss rate was recovered from the measurements of mass loss in a smaller pool-fire, 0.55 m diameter. This evolution is then normalized as:

$$\dot{\omega}(t) = \frac{\dot{m}(t)}{\overline{\dot{m}}} \quad (2)$$

where $\dot{\omega}(t)$ is the normalized instantaneous mass loss rate. Figure 4 shows the evolution of the normalized mass loss rate for the 0.55 m pan and for measurements for a wide range of pool-fire by Hostika *et al.* [11]. This comparison shows that the normalized mass loss rates for pool-fires in the range from 0.55 to 1.17 m diameter collapse in one curve. Each pool size shows a different burning time proportional to the initial volume of fuel in the pan. The normalized evolution was used to calculate the mass loss rate in each of the three fire tests and the heat release rate calculated using Eq. (1) and shown in Figure 5. The resulting steady-state heat release rates were 1.32 MW, 2.28 MW and 2.34 MW, respectively. The uncertainty associated with the heat released rate is estimated to be around ± 15 %.

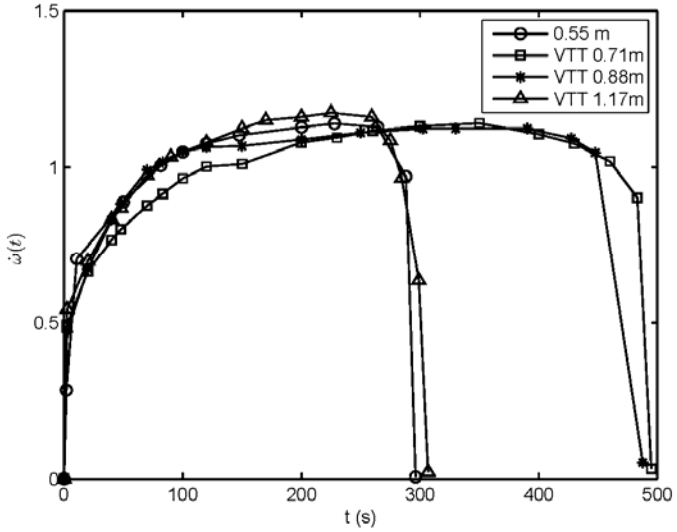

Fig. 4. Comparison of normalized mass loss rates, $\dot{\omega}(t)$, as measured for different heptane pool diameters. VTT results in [11].

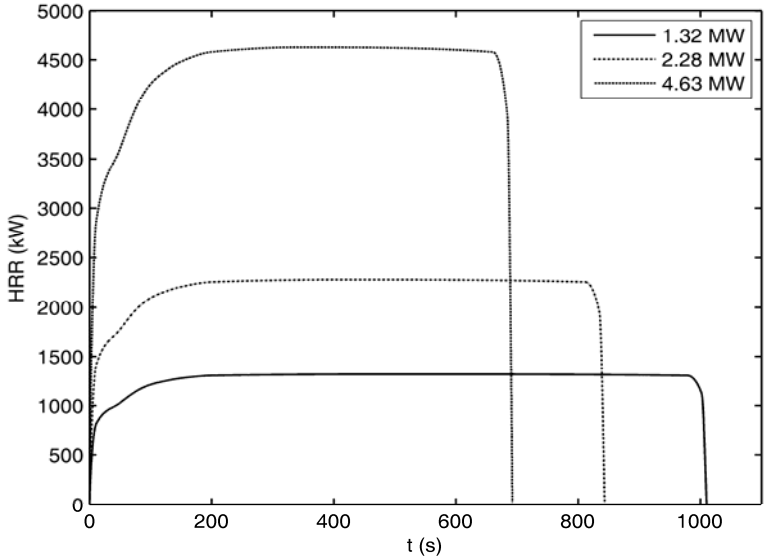

Fig. 5. Detail of the initial stage of the heat release rates estimated using Eq.(1) and the normalized mass loss rate from Eq. (2) shown in Figure 4.

As a verification of the tests, the flame height and the pulsation frequencies of the pool-fires were evaluated. The flame height was measured and compared with the empirical correlation for pool-fire from [7] seen in Eq. (3):

$$\frac{L}{D} = -1.02 + 3.7 \cdot \dot{Q}^{*2/5}, \tag{3}$$

where L is the flame height, D is the pool diameter, and $\dot{Q}^*$ is the Froude number of a fire defined as,

$$\dot{Q}^* = \frac{\dot{Q}}{\rho_\infty c_p T_\infty \sqrt{gD} D^2}, \tag{4}$$

where ρ_∞ and T_∞ are the ambient density and temperature, respectively, c_p is the specific heat of air and g is the gravity acceleration.

For Test 1, the flame height in the steady burning period was measured in the range 2.8 - 3.5 m, figure 6 a). This value agrees well with the prediction of 3.3 m for a 1.32 MW fire in a 0.92 m pan provided by Eq (3). The flame height of Test 2 ranged during the steady burning period from 3.8 m to 4.6 m, figure 6 b). This value agrees well with the prediction of 4.1 m from Eq. (3). The flame height of Test 3, figure 6 c), was similar to that in Test 2, ranging from 3.8 m to 4.6 m and agrees well with the prediction of 4.2 m.

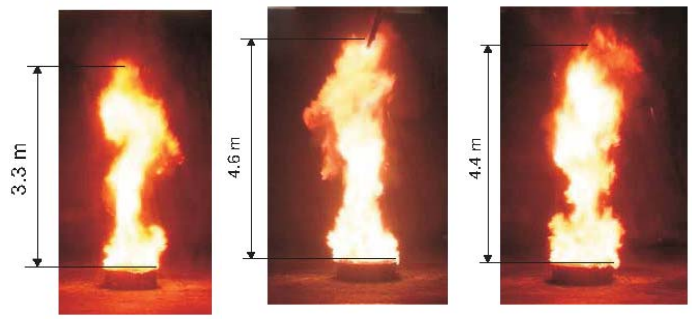

Fig. 6. Snapshot showing the flame heights during the steady-state of the tests. Test 1, 0.92 m pool and 1.32 MW fire in a), Test 2, 1.17 m pool and 2.28 MW fire in b), and Test 3, 1.17 m pool and 2.34 MW fire in c).

The pulsation frequencies of the two pool-fires used were visually estimated at their burning steady period by means of an image processing program. The estimations were compared with the theoretical values from two correlations. Cetegen and Ahmed [24] obtained the following expression for the frequency of the flame pulsation,

$$f = 1.5D^{-1/2} \text{ (Hz)}, \quad (5)$$

where D is the diameter of the pool-fire in m. Zukoski [25] suggests for the computation of this pulsation frequency,

$$f = [0.5 \pm 0.04]\left(\frac{g}{D}\right)^{1/2} \text{ (Hz)}, \quad (6)$$

which predicts values that include those obtained from the expression of Cetegen and Ahmed. Table 2 shows the theoretical and experimental values obtained for the pool-fires used with a really good agreement.

Frequency (Hz)	Pool-fire	
	D = 0.92 m	D = 1.17 m
Frequency Cetegen y Ahmed	1.56	1.39
Minimum Frequency Zukoski	1.50	1.33
Maximum Frequency Zukoski	1.76	1.56
Experimental Frequency	1.56	1.39

Table 2. Theoretical pulsation frequencies, in Hz, for the pool-fires used.

The complete set of measurements from the experiments is shown and discussed in section 5 of the paper, after the description of the fire simulations.

4.- Numerical Simulation

4.1.- Mathematical Model

Simulations of the three fire tests have been performed to compare with the experimental results. The CFD code used is FDS4 developed at NIST [14]. The code is widely used in fire protection engineering. The turbulence is modelled using a large-eddy simulation (LES) approach [26], and the combustion model is based on the mixture fraction approach that assumes the combustion is mixing-controlled. The radiative heat transfer is computed by solving the radiation transport equation for a non-scattering grey gas.

The computational domain includes the atrium space, the walls and the roof. The heat release rate is prescribed in the input as a function of time following the results in Figure 5. The radiative fraction is set to 0.35 which is the value experimentally measured for similar heptane fires [10, 27]. The grilled vents and inactive exhaust fans have been simulated as openings to the atmosphere at ambient pressure. The active exhaust fans were simulated as vents with a constant velocity across their area providing the nominal flow rate of 3.8 m^3/s

specified by the manufacturer. The walls and roof were modelled as steel sheets (density of 7800 kg/m^3, thermal conductivity of 45 W/K m, specific heat of 460 J/kg K and emissivity of 0.3 [28]) with a thickness of 6 mm. The floor is modelled as a thick layer of concrete (density of 1860 kg/m^3, thermal conductivity of 0.72 W/K m, specific heat of 780 J/kg K [28]). Other parameters in FDS4 have been left as the default values.

4.2.- Grid Sensitivity Study

The grid used is one of the most important numerical parameter in CFD [14] dictating its numerical accuracy. The necessary spatial resolution for a proper LES simulation is customary defined in terms of the characteristic diameter of a plume [19], which is defined as [7],

$$z^* = \left(\frac{\dot{Q}}{\rho_\infty c_{p,\infty} T_\infty \sqrt{g}} \right)^{2/5}. \qquad (7)$$

The resolution R^* of a numerical grid is defined as,

$$R^* = \frac{\Delta x}{z}, \qquad (8)$$

where Δx is the characteristic length of a cell for a given grid. The necessary resolution suggested in most studies is between 1/5 and 1/10 [19, 14]. Other studies [29] suggested resolution of 1/20 to successfully predict the flame height. For this work, a resolution between 1/10 and 1/15 has been chosen, which results in the number of grid cells shown in Table 3.

Fire test (MW)	Cells number for R^* = 1/5	Cells number for R^* = 1/10	Cells number for R^* = 1/15
1.32	83	167	250
2.28	67	135	202
2.34	67	133	200

Table 3. Number of cells needed in each direction for different grid resolutions.

In the grid sensitivity studies conducted here, the size of the cells in the grid has been systematically reduced until a compromise solution between numerical accuracy and computational time is achieved. Six grids have been studied, 40 cells, 60, 90, 120, 150 and 180 cells per side of the cubic atrium (*i.e.* 20 m). For the sake of simplicity, the grid sensitivity study has been conducted with steady-state fires at two heat release rates (1.3 and 2.3 MW). The heat release rate is set constant and 100 s are simulated for each grid size. Then, the temperatures have been averaged for the last 80 s at each height of interest. Results have been compared between them to quantify grid independence. In LES is not possible to archive perfect grid independence although little variations can be theoretically expected

between grids if they are fine enough [26, 30]. Tables 4 and 5 show the temperature predictions in the atrium for each grid. The plume temperature at 5 m high varies considerably with the grid size. This location is sometimes reached by the flame and is not expected to be accurate due to the difficulties of modelling accurately the near field of a flame using FDS4 [14]. For both fire powers, the temperatures at 13 m high and at the exhaust fans vary significantly for the three coarser grids, while it is fairly independent for grids finer than 120 cells per side of the atrium. This is equivalent to cubic cells smaller than 0.17 m in length. It is concluded then that finer grids than this one are not required in order to capture the far field temperature high in the atrium but will only increase the computing time required.

Height	Temperature predictions (ºC)						Relative error respect to finest grid (%)				
	40 cells	60 cells	90 cells	120 cells	150 cells	180 cells	40 cells	60 cells	90 cells	120 cells	150 cells
Exhaust fan	49	66	64	53	58	56	13	18	14	5	4
Plume at 13m	64	110	99	78	81	74	14	49	34	5	9
Plume at 9m	80	152	173	129	160	136	41	12	27	5	18
Plume at 5m	116	226	333	293	503	487	76	54	32	40	3

Table 4. Centreline plume temperatures at different heights as a function of the grid size for a 1.3 MW fire. Grids are expressed as number of cells per atrium side (20 m).

Comparison of the results for different grids shows that the relative error between grids is big for the three coarser ones. For the 1.3 MW fire, the relative errors between the finer grids of 150 cells per side and 180 cells per side are lower than 10 % at 13 m high, and lower than 5 % at the exhaust fans. For the 2.3 MW fire, the discrepancy between the finer grids is lower than 20 % and 5 %, respectively. Thus, it is concluded that any of the two finer grids is valid for simulating the fire. Taking into account the criterion of special resolution between 1/10 and 1/15, the 180 cells per side was chosen for the 1.3 MW fire and the 150 cells per side for the 2.3 MW fire.

Height	Temperature predictions (ºC)						Relative error respect to finest grid (%)				
	40 cells	60 cells	90 cells	120 cells	150 cells	180 cells	40 cells	60 cells	90 cells	120 cells	150 cells
Exhaust fan	58	72	67	60	59	56	4	29	20	7	5
Plume at 13m	110	126	111	114	88	75	47	68	48	52	17
Plume at 9m	143	193	221	262	200	142	1	36	56	85	41
Plume at 5m	174	259	448	582	646	540	68	52	17	8	20

Table 5. Centreline plume temperatures at different heights as a function of the grid size for a 2.3 MW fire. Grids are expressed as number of cells per atrium side (20 m).

Additionally, and to verify that the grids are fine enough to provide accurate results, the results have been compared with the values from plume theory provided in [31]. Table 6 shows the relative errors for each grid and fire sizes. It is seen that the predictions agree better

with the plume correlation for finer grids and at higher locations. Close to the flame, the agreement is poor. Figure 7 shows the results contained in Tables 4 and 5, and predictions from plume theory. It shows that the coarser grids do not predict well the plume temperature. It is not until the grid of 90 cells per side that some agreement can be appreciated. The two finest grids show the largest agreement with plume theory. The grids of 150 cells and 180 cells per side over-predict plume temperature near the flame (5 m high). They also over-predict plume temperature below 9 m high. The over-prediction is reduced at the upper parts of the atrium, which are the most important for smoke evacuation in atria, showing good agreement. It is concluded then that the selected grids of 150 and 180 cells per side provide good accuracy with an error smaller than 10 % above 13 m from the ground as compared to the plume correlations.

	Relative error respect to plume correlation (%)											
Height	**1.3 MW**						**2.3 MW**					
(m)	**40 cells**	**60 cells**	**90 cells**	**120 cells**	**150 cells**	**180 cells**	**40 cells**	**60 cells**	**90 cells**	**120 cells**	**150 cells**	**180 cells**
5	59.5	21.0	16.7	2.7	76.4	70.5	57.0	36.1	10.4	43.4	59.2	33.1
9	30.0	33.6	51.6	12.8	42.3	18.5	0.3	35.2	54.8	83.2	41.5	1.3
13	11.9	51.0	35.5	6.5	12.2	0.4	34.4	53.1	36.1	40.0	10.1	9.7
17	13.1	16.2	13.9	6.2	2.5	1.1	1.1	24.7	15.5	2.4	2.5	4.9

Table 6. Relative errors in the centreline plume temperature respect to plume correlation [31]. Grids are expressed as number of cells per atrium side (20 m).

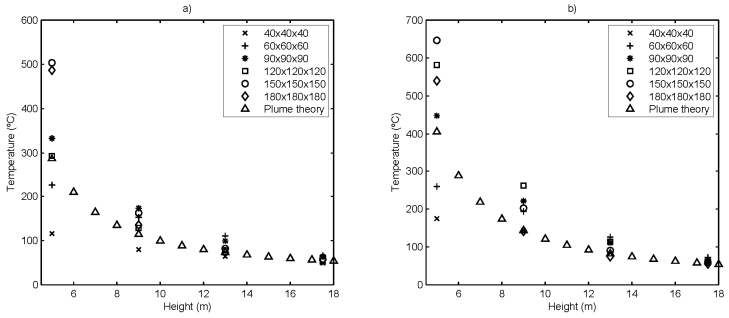

Fig. 7. Comparison of predicted plume temperatures for different grid sizes for the 1.3 MW fire in a), and for the 2.3 MW fire in b).

5.- Results

At present section, experimental results from the three Fire Tests as well as comparison with predicted results from FDS are presented and discussed. Results in three key regions are reported: the plume temperature, the exhaust smoke temperature, and the smoke layer temperature by means of the temperature of the air close to the walls. The smoke layer height in the experiments is calculated using the N-percent method [32].

Figures 8, 10 and 12 report the temperatures of the plume for both 3 mm bared (sensors 24, 28, 31) and sheathed (sensors 26, 30 and 32) thermocouples measurements. In general, the agreement between both thermocouple types is good (lower than 10 %). This fact reflects on the accuracy of the measurements and their reliability.

Next, each of the fire tests is discussed separately.

- **Test 1:**

This test is with the pool-fire of 0.92 m, with a HRR of 1.3 MW. Two fans on the roof were activated (E2 and E4) and the other two were inactive (E1 and E3) but their opening acted as vents for natural ventilation. The vents were 100 % open with symmetric layout. Figures 8 and 9 show the measurements and predictions vs. time. Figure 8 compares results for the plume temperature at central line of the atrium and at the exhaust fans, and figure 9 does for the near the walls region and for the smoke layer height. This figure layout will be followed in next tests.

This test presented high spatial symmetry due to the ambient conditions were really steady and calm, e.g. the wind speed was null, and did not influence the fire. This can be deduced from the temperature measurements at the lower heights at the centreline, h = 4.55 m and h = 8.55 m high, where the temperatures are relatively constant, figures 8 a) and b), from t = 200 s. This reflects that the plume did not suffer any strong deviation. In addition, at these locations, it can be clearly appreciated the initial transient stage of the heptane combustion. At both heights, the temperature rises progressively up to reaching a constant value around t = 200 s, when a constant HRR is reached. At h = 12.55 m high at the centreline, the temperature rises continuously, figure 8 c). As commented before, when the smoke from the plume reaches the ceiling starts to accumulate forming the smoke layer height. When it reaches the height of 12 m, there is no more fresh ambient air entrainment at the plume from that height. Instead, there is hot smoke entrainment at the plume, which increases the plume temperature. At t = 400 s, it reaches T = 70 ºC and rises slowly up to T = 79 ºC at the end.

The temperature at the exhaust fans, figure 8 d), shows that the smoke reaches the ceiling about 10 s after ignition. Then, it starts to accumulate, the smoke temperature increases slowly and continuously to T = 75 ºC, and after t = 850 s, it reaches quasi steady-state.

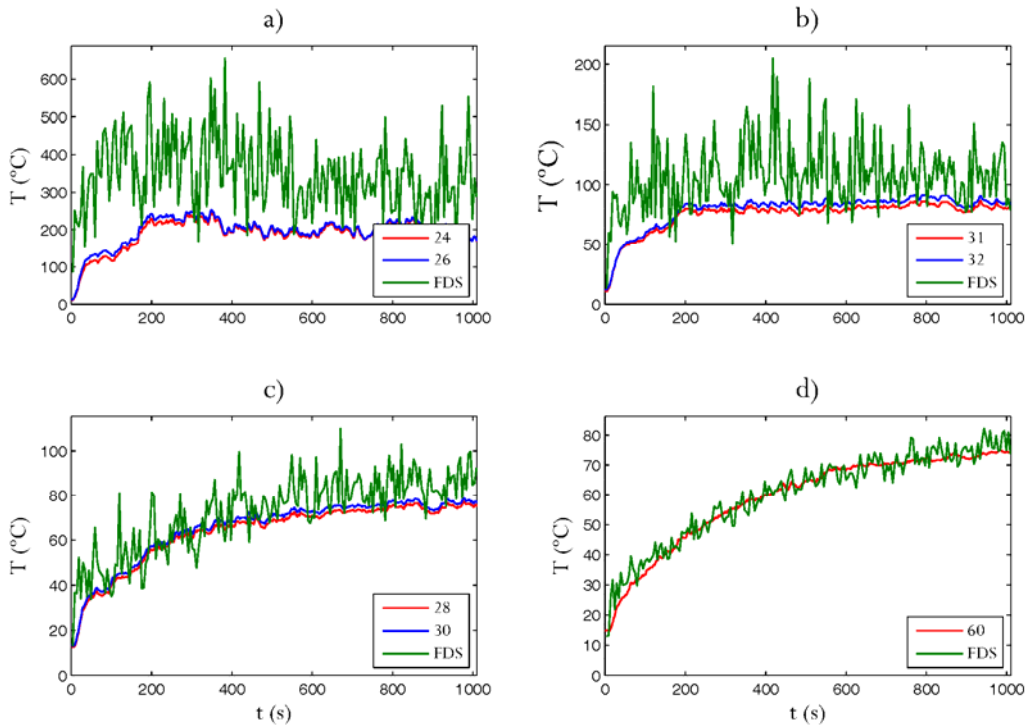

Fig. 8. Temperature measurements and predictions at the plume and exhaust fans for Test 1. 4.55 m high in a); 8.55 m high in b); 12.55 m high in c); Exhaust fan in d). Measurements are for both bare and sheathed thermocouples and identified by sensor number according to figure 3.

Figure 9 shows temperature results near the wall for walls A and C. They show the built up of the hot layer. This is due to the smoke exhaust rate at the top being lower than the flow along the plume at the roof height. The temperature rises first at h = 15 m high at t = 25 s, as the ceiling jet reaches first this location. Then, the smoke layer continues growing, and the temperature starts to rise at the height of h = 10 m at t = 80 s and, finally, at the one of h = 5 m at t = 100 s. Comparison of the measurements at symmetrical wall position shows a strong spatial symmetry since the evolution is almost identical. This observation implies that the plume and the smoke layers were not affected by flow perturbations during the test. As commented before, the smoke layer height has been calculated, figure 9 d), applying the N-percent method [32], and compared with the one predicted by FDS. It has been assumed different values for N, 10 % and 20 % as in [32] and 30 % as in [33]. It is observed that after 200 s the smoke layer reaches the height of 5 m for the most conservative assumption, whereas this location is not reached for the least conservative one. The temperature values registered at the exhaust fans, T = 75 ºC, at h = 15 m, T = 68 ºC, at h = 10 m high, T = 66 ºC, and at h = 5 m high near the wall, T = 28 ºC, show the strong thermal vertical stratification of the smoke layer. In addition, the differences between the two higher locations of the near the wall region and the lowest one, 40 ºC (60 %), indicate that the smoke layer hardly reaches or does not reach the last location.

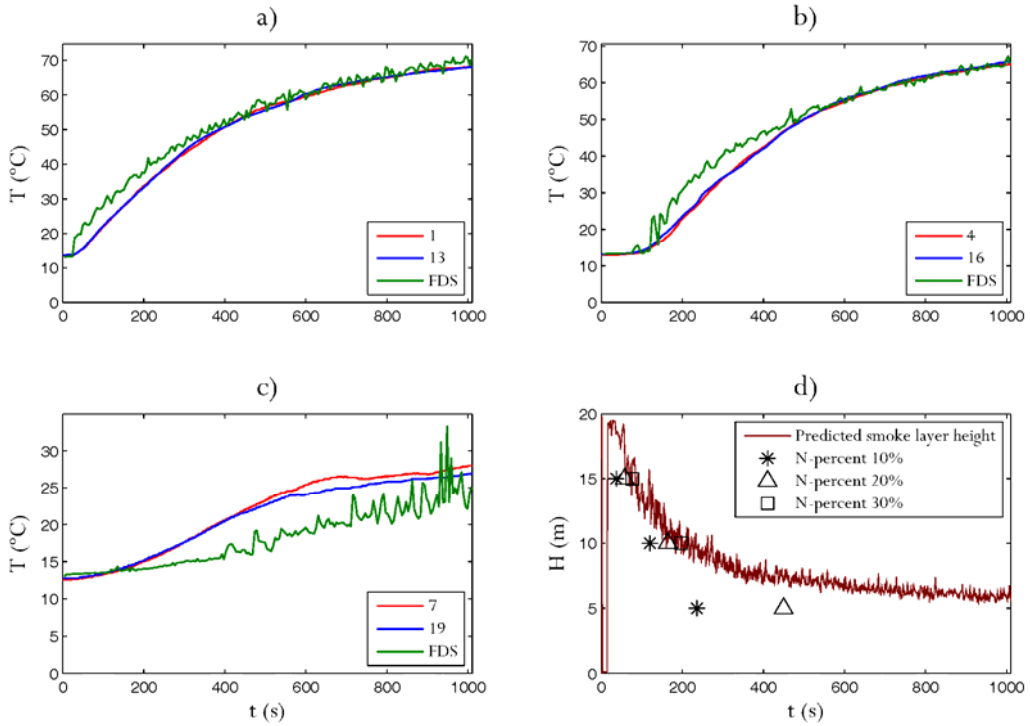

Fig. 9. Temperature near the walls and smoke layer height measurements and predictions for Test 1. Temperatures 15 m high in a); 10 m high in b); 5 m high in c); and smoke layer height in d). Measurements are for symmetrical locations at walls A and C and identified by sensor number according to figure 3.

The numerical simulation did not present any perturbation and the fire dynamics evolved normally. In the near field, FDS predicts the same temperature trends that those observed from the measurements, that is, relative constant temperature at h = 4.55 m and h = 8.55 m high at the centreline and continuous temperature rise at h = 12.55 m high. Numerically, the temperature near the flame fluctuates strongly whereas, experimentally, the high frequencies harmonics are filtered by the thermocouples. FDS over-predicts the plume temperature near the flame and the lower plume heights. The bigger discrepancies are observed at the fire growth period. FDS predicts a faster temperature rise than the one measured at the experiments. These moments present higher scattering as the mass loss rates varies significantly. When a constant HRR is reached (t = 200 s), the agreement improves and the differences reduce with height. The relative error at h = 4.55 m, figure 8 a), ranges from 40 to 50 %, at h = 8.55 m, figure 8 b), is 20 %, within the error associated to FDS, and at h = 12.55 m, figure 8 c), is lower than 10 %.

In the far field, FDS predicts better the fire-induced conditions. At the exhaust fans, the agreement is really good, figure 8 d), where no difference is observed. At upper parts of the near the walls region, the agreement is also good, figure 9 a) and b), with a perfect match from t = 400 s, approximately. There are some differences at the initial moments, when FDS predicts faster temperature rises than those obtained experimentally. This influences the predictions at h = 5 m high near the wall. At that location, experimentally the temperature rises up to T = 26 ºC at t = 650 s. Then, the temperature remains almost constant until the end.

Numerically, FDS does not predict any temperature rise initially. Only at the end, FDS predicts certain temperature rise. It could happen that, initially, FDS predicts an excessive smoke accumulation at the upper parts, caused by a smoke temperature over-prediction at those locations which enhances its buoyancy and which reduces the smoke layer descent velocity. However, in general the predictions of smoke layer height, figure 9 d), agree well with measurements during most of the growth period although a longer time to reach the height of h = 5 m is predicted.

The outer conditions, e.g. outer wind, affect the inside fire-induced conditions. FDS predicts well the fire-induced conditions when no outer conditions are influencing. However, as it will be showed in next tests, the no simulation of these effects generates noticeable differences between experiments and simulations at the near field region when they are important.

- **Test 2:**

This test is with the pool-fire of 1.17 m, with a HRR of 2.3 MW. Two fans on the roof were activated (E2 and E4) and the other two were inactive (E1 and E3) acting as vents for natural ventilation. The vents were 100 % open with symmetric layout. Figures 10 and 11 show the measurements and predictions vs. time.

This test was carried out immediately after the previous one. Thus, the outer conditions were similar, see table 1. The wind was blowing softly and, thus, there were little outer perturbations that slightly affected the flame verticality. The plume temperature at h = 4.55 m, figure 10 a), and at h = 8.55 m, figure 10 b), varied slightly during the test, indicating some small plume deviations caused by ventilation asymmetries induced by the outer wind. At this point, two moments could be highlighted, at t = 135 s, when the temperature drops at h = 4.55 m high at the centreline, and at t = 400 s, when the temperature drops again at the same location. These perturbations hardly affect the next location, h = 8.55 m high at the centreline, indicating that these flame inclinations were not very strong. Thus, these perturbations can be considered negligible, as the temperature evolution at h = 12.55 m high at the centreline or at the far field do not present any perturbation.

Figure 10 d) shows the smoke temperature at the exhaust fans, which reaches the roof about t = 8 s after ignition. The smoke then accumulates at the top forming a smoke layer. The smoke temperature at the exhaust fans rises to T = 110 ºC, reaching a quasi steady-state at t = 650 s.

Figure 11 shows temperature results near the walls A and C. Again, the high symmetry of the test can be deduced from the temperature measurements at the near the walls region, figures 11 a), b) and c). The heat release rate of this test is larger than in Test 1. Thus, the smoke production is also larger and the hot smoke layer grows faster. As the smoke layer grows, the temperature starts to rise at the height of h = 15 m before t = 20 s, reaching a quasi steady-state at 700 s, when T = 98 ºC. The temperature starts to rise at the height of h = 10 m at t =

40 s, reaching a maximum value of T = 96 ºC. At this location, the slope of the temperature measurement at the end shows a rising trend. Thus, although quasi-steady conditions were nearly reached at the two higher locations of the near the wall region, the fire conditions were still evolving at lower zones. The temperature starts to rise at the height of h = 5 m about t = 60 s after ignition. At this location, the temperature rises fast up to T = 39 ºC, at t = 460 s. From then on, the temperature rises slowly to T = 44 ºC, indicating the inside conditions were stabilizing and the smoke layer height was reaching a steady value. The smoke layer reaches this height for all the N-values, being before t = 200 s for the most conservative assumption. However, the large temperature difference between h = 15 m and h = 10 m high and h = 5 m high, 54 ºC (55 %), indicates that the smoke layer boundary has to be very close to the last.

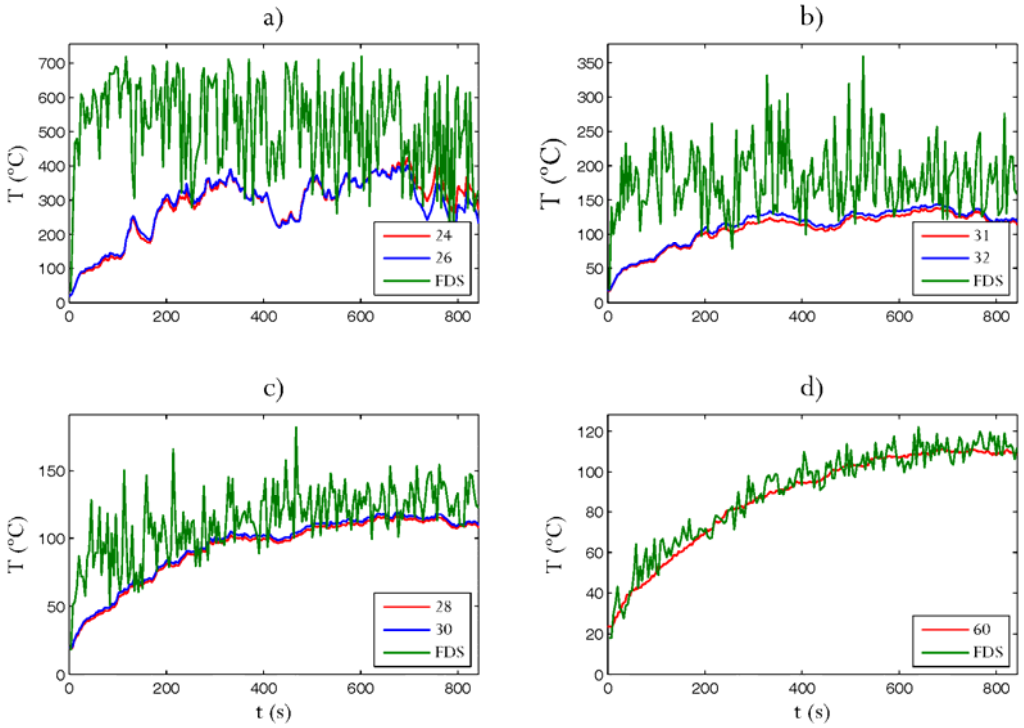

Fig. 10. Temperature measurements and predictions at the plume and exhaust fans for Test 2. 4.55 m high in a); 8.55 m high in b); 12.55 m high in c); Exhaust fan in d). Measurements are for both bare and sheathed thermocouples and identified by sensor number according to figure 3.

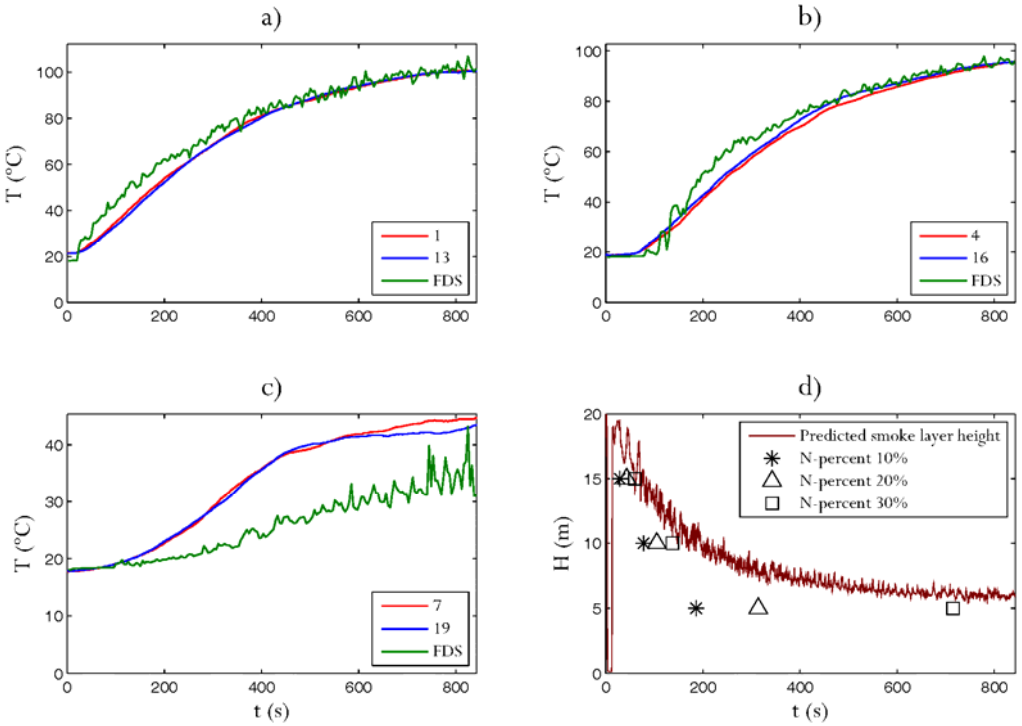

Fig. 11. Temperature near the walls and smoke layer height measurements and predictions for Test 2. Temperatures 15 m high in a); 10 m high in b); 5 m high in c); and smoke layer height in d). Measurements are for symmetrical locations at walls A and C and identified by sensor number according to figure 3.

Numerically, the plume temperatures predicted by FDS are higher than measurements. Again, the main largest differences are found at the beginning of the fire test as happened in the previous test. At these moments, FDS predicts a much faster temperature rise than the one observed experimentally. Regardless of these first moments, the maximum relative errors between experiments and FDS predictions range from 50 % to 80 % at h = 4.55 m, figure 10 a), are equal to 40 % at h= 8.55 m, figure 10 b), and lower than 12.5 %, within FDS accuracy, at h = 12.55m, figure 10 c). This last location could be considered to be at the near field region which is normally not well predicted by CFD models. However, the agreement achieved with FDS is quite good, which reflects the accuracy of the code. At the exhaust fans, figure 10 d), FDS agrees totally with the temperature measurements, with no differences. At the upper parts of the near the walls region, that is, at the heights of h = 15 m, figure 11 a), and h = 10 m, figure 11 b), there is also good agreement between measurements and predictions. Again, FDS predicts a faster temperature rise at the initial moments with differences lower than 30 %, at h = 15 m high, and lower than 20 % at h = 10 m high. From t = 400 s, the predicted values match perfectly with the measurements. At h = 5 m high near the wall, FDS under-predicts air temperature, figure 11 c), with relative error lower than 25 % at the end. Thus, FDS slightly over-predicts the smoke layer height. Despite these differences, predictions of smoke layer height agree well with measurements for a value of N = 30 %.

- **Test 3:**

Test 3 is with the pan of 1.17 m. The four fans on the roof were inactive; thus, only natural ventilation was considered. Figures 12 and 13 show the measurements and predictions vs. time.

Figure 12 compares results for the plume at central line of the atrium and at the exhaust fans. This fire test shows relatively constant temperatures at the lower heights, figures 12 a) and b), at the steady combustion period. This indicates little plume deviations due to ventilation asymmetries. At the end, small plume temperature drop is observed at the lowest height, figure 12 a), due to the effect of the wind. Temperature starts to rise at the exhaust fans, figure 12 d), 8 s after ignition. Then, smoke starts to accumulate. The absence of mechanical ventilation causes faster smoke accumulation than in the previous test and higher smoke temperatures. After 700 s the smoke temperature reaches a quasi steady-state at 120 ºC.

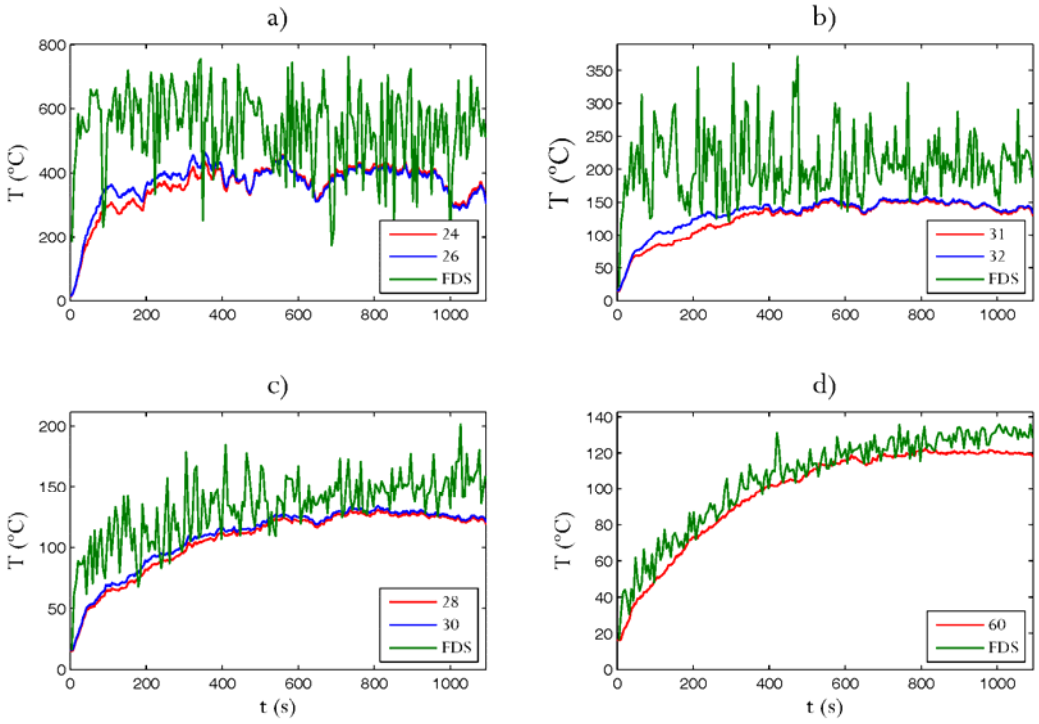

Fig. 12. Temperature measurements and predictions at the plume and exhaust fans for Test 3. 4.55 m high in a); 8.55 m high in b); 12.55 m high in c); Exhaust fan in d). Measurements are for both bare and sheathed thermocouples and identified by sensor number according to figure 3.

Figure 13 shows temperature results near the walls. High spatial symmetry is found. Due to faster accumulation of smoke the temperature increase is larger near the walls. Temperature rises first at 15 m, figure 13 a), high up to 110 ºC at the final moments. Smoke reaches later the height of 10 m, figure 13 b), and temperature rises to a value of 104 ºC. The larger accumulation of smoke can be noticed at 5 m high, figure 13 d). Temperature rises up to a maximum value of 68 ºC, at 700 s. Then, it drops to 60 ºC remaining constant until the end.

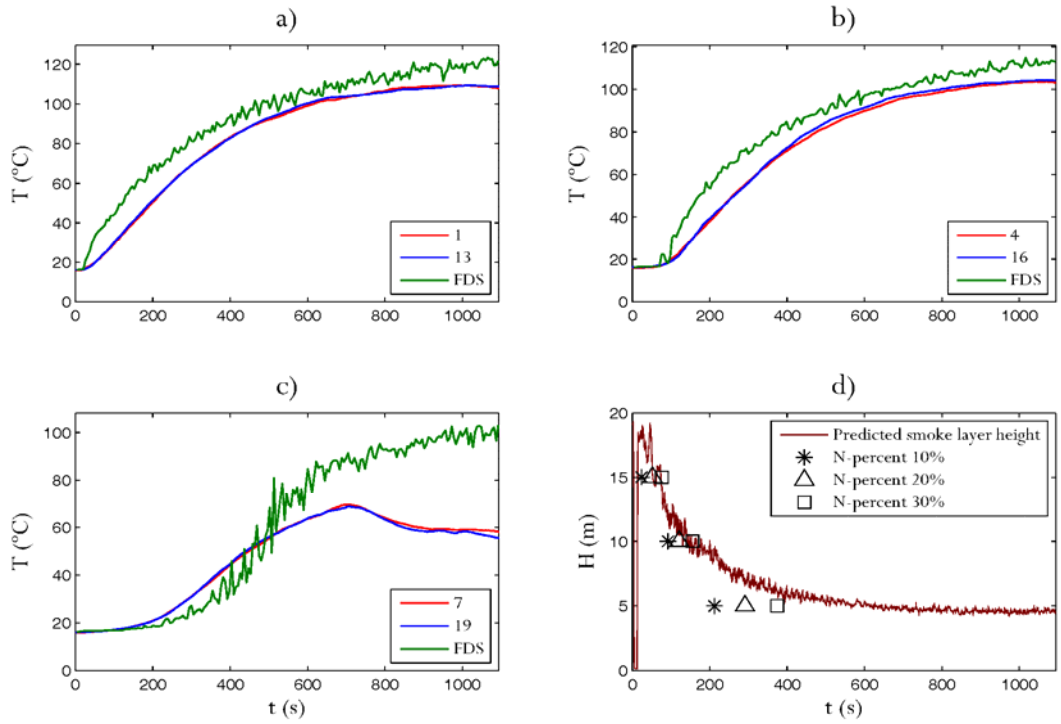

Fig. 13. Temperature near the walls and smoke layer height measurements and predictions for Test 3. Temperatures 15 m high, in a); 10 m high, in b); 5 m high, in c); and smoke layer height in d). Measurements are for symmetrical locations at walls A and C and identified by sensor number according to figure 3.

Comparison with simulation shows that the plume temperatures predicted are higher than the measurements, figures 12 a), b) and c). The differences are larger at the lower parts, figures 12 a) and b). The relative error at h = 4.55 m, figure 12 a), ranges from 50 to 80 %, at h = 8.55 m, figure 12 b), from 35 to 45 %, and at h = 12.55 m, figure 12 c), from 20 to 25 %. Natural ventilation is more influenced by outer effects (e.g. wind) than mechanical exhaust. Thus, larger differences between measurements and predictions than in previous test might be expected. At the exhaust fans, figure 12 d), the predicted smoke temperature agrees well with measurements, being the relative error lower than 20 %. The numerical simulation slightly over-predicts the temperatures near the walls. For h = 15 m, figure 13 a), and h = 10 m, figure 13 b), still good agreement is found, with relative errors lower than 15 %, at h = 15 m, and lower than 10 %, at h = 10 m, during the steady combustion period. Higher differences are found at h = 5 m, figure 13 c). The agreement is good until 500 s. Then, the numerical simulation predicts temperature increase until the end whereas experimentally the smoke temperature rises slowly and drops at 700 s to 60 ºC, remaining constant. The largest differences are found at the end, when the relative error grows up to 65 %. This is due to the lowest parts are most sensitive to flow perturbations and they have not been simulated numerically. Good agreement is found between smoke layer height predictions and measurements.

The predicted smoke layer height has been compared with the experimental results using the N-percent method [32]. A temperature increase from ambient temperature of 10 – 20 % of the highest temperature rise has been typically been used to define the base of the transition zone between the smoke layer and the cold layer [32]. Other authors [33] locate the smoke layer where the temperature increase is of 30 % of the highest temperature rise in atria. In general, there is good agreement between FDS predictions and the 30 % temperature increase. It is observed that the simulations slightly overestimate the final smoke layer height. This is in agreement with other works [33].

6.- Conclusions

The two main objectives of the present work were to generate a set of experimental data of full-scale atrium fires and to check the capability of FDS to predict the inner fire-induced conditions.

First, results from experiments carried out at the “Fire Atrium” of the Centro Tecnológico del Metal, in Murcia, have been presented. Two different fire sizes (pool-fires of D = 0.92 m and D = 1.17 m) and two different smoke exhaust methods (mixed venting conditions and natural ventilation) have been tested. Additionally, special interest has been focused on plume temperature as these measurements are the most challenging ones.

Second, FDS simulations have been performed to check the code capability for predicting the fire-induced conditions. A grid resolution, R^*, between 1/10 y 1/15 has been chosen for each simulation. With this grid resolution it has been observed that FDS simulations over-predict plume temperature near the flame, h = 4.55 m and 8.55 m. This has been also found in other works [19]. This is a challenging prediction because the temperature decreases rapidly just above the flame tip. Nevertheless, the objective of these simulations was to check the capability of FDS to predict the fire far field. It has been observed that FDS slightly over-predicts the plume temperature at h = 12.55 m, normally within the range of accuracy associated to the own code, 5 % to 20 % [14]. At the exhaust fans and the upper parts near the wall, h = 15 m and h = 10 m, FDS predictions agree really well with experimental results. At the lowest height near the wall, h = 5 m, discrepancies between measurements and predictions have been found. This trend has been also observed in other works [34].

Finally, the discrepancies between experiments and predictions become larger when not so controlled fires are simulated. This is, when there are bigger differences between the real and the simulated boundary conditions. This can be noticed at the fire test with only natural ventilation. In this case, the ventilation is not so controlled than at the rest. As natural ventilation has been used in this fire test the ambient conditions influence much more, e.g. outer wind, and can not been implemented in FDS. Another source of discrepancies between experiments and predictions could be the differences found at the vents and exhaust fans implementation. The real vents are grilled and can generate little pressure losses that have not

been implemented numerically. The exhaust fans have been implemented as outflow velocities, the ones that are on, and as openings, the ones that are off. Again, little pressure losses have not been taken into account numerically. Despite the discrepancies between experiments and predictions FDS has turned out to be suitable to simulate this kind of fires in big volume buildings.

Acknowledgements

The authors want to acknowledge the Centro Tecnológico del Metal of Murcia for the use of their test rig, the Professor J. L. Torero, T. Steinhaus, C.Abecassis-Empis, P. Reszka, W. Jahn, from the University of Edinburgh, for their technical suggestions and supervision. Simulations have been carried out at the computational facilities of the Technological Research Services of the Technical University of Cartagena (SAIT) and the University of Jaen. This work has been supported by Ministerio de Educación y Ciencia of Spain (Projects CT/G30572473, and FIT-020700-2004-25 and grant TRA2006-15015) and by the Junta de Andalucía of Spain (Project number P07-TEP-02693).

References

[1] Cox G., Fire Research in the 21st Century, Fire Safety Journal, 32, 1999a, pp. 19-203.

[2] Tieszen, S.R., On the Fluid Mechanics of Fires, Annu. Rev. Fluid Mech., 33, 2001, pp. 67-92.

[3] Saxon, R. The atrium comes of age, Longman, London, 1994.

[4] NFPA 92B. Standard for Smoke Management Systems in Malls, Atria and Large Spaces. National Fire Protection Association: Quincy, MA, 2005.

[5] Nam, S. Actuation of sprinklers at high ceiling clearance facilities. Fire Safety Journal, 2004, vol. 39, 619–642.

[6] Drysdale, D. An introduction to fire dynamics. 2nd Ed. 2007. John Wiley & Sons, University of Edinburgh, UK.

[7] SFPE Handbook of Fire Protection Engineering. 3rd Ed.; National Fire Protection Association: Quincy, Ma, 2002.

[8] Tanaka, T.; Yamana, T. Smoke control in large scale spaces - Part 1. Fire Science and Technology, 1985, vol. 5 (1), 31–40.

[9] G. Cox, Some recent progress in the field modelling of fire. In Fire Science and Technology, Proceedings of the First Asian Conference (Edited by W. Fan and Z. Fu), pp. 5&59, International Academic Publisher, Beijing (1992).

[10] Chow, W.K.; Li, Y.Z.; Cui, E.; Huo, R. Natural smoke filling in atrium with liquid pool-fires up to 1.6 MW. Building and Environment, 2001, vol. 36, 121-127.

[11] Hostikka, S.; Kokkala, M.; Vaari, J. Experimental study of the localized room fires.NFSC2 Test Series, VTT Research Notes 2104; Technical Research Centre of Finland: Finland, 2001.

[12] Fang, L.; Nielsen, P.V.; Brohus, H. Investigation on smoke movement and smoke control for atrium in green and sustainable buildings, Department of Civil Engineering, Technical Report No. 32; Aalborg University: Aalborg, Denmark, 2007.

[13] Quintiere, J.G. Scaling applications in fire research. Fire Safety Journal 1989; 15: 3-29.

[14] McGrattan, K. Fire Dynamics Simulator (Version 4) Technical Reference Guide. Ed.,National Institute of Standards and Technology, Special Publication 1018, 2004.

[15] SMARTFIRE V4.1. User Guide and Technical Manual, 2008.

[16] SFPE Engineering Guide to Performance-based Fire Protection; Second Edition; National Fire Protection Association (NFPA): Quincy, MA, 2007.

[17] Qin, T.X.; Guo, Y.C.; Chan, C.K.; Lin, W.Y. Numerical simulation of the spread of smoke in an atrium under fire scenario. Building and Environment, 2009, vol. 44, 56–65

[18] Kerber, S.; Milke, J.A. Using FDS to Simulate Smoke Layer Interface Height in a Simple Atrium Fire Technology, 2007, vol. 43, 45–75.

[19] Verification and Validation of Selected Fire Models for Nuclear Power Plant Applications. NUREG-1824 Final Report; U.S. Nuclear Regulatory Commission, Office of Nuclear Regulatory Research: Palo Alto, CA, 2007.

[20] Rein, G.; Zhang, X.; Williams, P.; Hume, B.; Heise, A.; Jowsey, A.; Lane, B.; Torero, J.L. Multi-story Fire Analysis for High-Rise Buildings. Proceedings of the 11th International Interflam Conference: London, 2007.
http://hdl.handle.net/1842/1980

[21] Gutiérrez-Montes, C., Sanmiguel-Rojas, E., S. Kaiser, A., Viedma, A. Numerical model and validation experiments of atrium enclosure fire in a new fire test facility. Building and Environment, 2008, 43 (11), pp: 1912–1928.

[22] Welch, S., Jowsey, A., Deeny, S., Morgan, R., Torero, J.L. BRE large compartment fire tests—Characterising post-flashover fires for model validation. Fire Safety Journal 42 (2007) 548–567.

[23] Tewarson, A. Combustion efficiency and its radiative component. Fire Safety Journal, 2004, 39, pp. 131-141.

[24] Cetegen, B.M., Ahmed, T.A. Experiments on the periodic instability of buoyant plumes and pool-fires, Combustion and Flame, 1993, 93, pp. 157–184.

[25] Zukoski, E.E. Properties of fire plumes, in Combustion Fundamentals of Fire; Editor, Cox, G.; Academic Press: London, 1995.

[26] Pope, S.B. Computations of turbulent combustion: progress and challenges. Proceedings of the Combustion Institute, 1990, 23, pp. 591-612

[27] Hamins, A., Klassen, M., Gore, J. Kashiwagi, T. Estimate of Flame Radiance via single Location Measurement in Liquid Pool Fires Combustion and Flame, 86, 223-228, 1991.

[28] Incropera, F. P., DeWitt, D. P., Fundamentals of Heat and Mass Transfer. John Wiley & Sons; 4 Sub-edition , 1996

[29] Ma, T.G., Quintiere, J.G. Numerical simulation of axi-symmetric fire plumes: accuracy and limitations. Fire Safety Journal, 2003, 38; pp.467-492.

[30] McGrattan, K.B., Baum, H.R., Rehm, R.G. Large Eddy Simulations of Smoke Movement. Fire Safety Journal, 1998, 30, pp. 161-178.

[31] Heskestad, G. Engineering Relations for Fire Plumes. Fire Safety Journal, 1984, 7, pp. 25-32.

[32] Cooper, L.Y., Harkleroad, M., Quintiere, J., Reinkinen, W. An experimental study of upper hot layer stratification in full-scale multi-room fire scenarios. Journal of Heat and mass transfer, 1982; 104 pp. 741-749.

[33] Yi, L.; Chow, W.K.; Li, Y.Z.; Huo, R. A simple two-layer zone model on mechanical exhaust in an atrium. Building and Environment, 2005, vol. 40, 869–880.

[34] Rinne, T., Hietaniemi, J., Hostikka, S. Experimental validation of the FDS simulations of smoke and gas concentrations. ESPOO 2007, VTT WORKING PAPERS 66.